Pflügers Arch – Eur J Physiol (1997) 434:615–631

INSTRUMENTS AND TECHNIQUES

Ariel L. Escobar · Patricio Velez · Albert M. Kim
Fredy Cifuentes · Michael Fill · Julio L. Vergara

Kinetic properties of DM-nitrophen and calcium indicators: rapid transient response to flash photolysis

Received: 17 March 1997 / Received after revision and accepted: 16 May 1997

Abstract We describe a high temporal resolution confocal spot microfluorimetry setup which makes possible the detection of fluorescence transients elicited by Ca^{2+} indicators in response to large (50–200 μM), short duration (<100 ns), free [Ca^{2+}] transients generated by laser flash photolysis of DM-nitrophen (DM-n; caged Ca^{2+}). The equilibrium and kinetic properties of the commercially available indicators Fluo-3, Rhod-2, CalciumOrange-5N (COr-5N) and CalciumGreen-2 (CGr-2) were determined experimentally. The data reveal that COr-5N displays simple, fast response kinetics while, in contrast, Fluo-3, Rhod-2 and CGr-2 are characterized by significantly slower kinetic properties. These latter indicators may be unsuitable for tracking Ca^{2+} signaling events lasting only a few milliseconds. A model which accurately predicts the time course of fluorescence transients in response to rapid free [Ca^{2+}] changes was developed. Experimental data and model predictions concur only when the association rate constant of DM-n is approximately 20 times faster than previously reported. This work establishes a quantitative theoretical framework for the study of fast Ca^{2+} signaling events and the use of flash photolysis in cells and model systems.

Key words Caged calcium · Calcium indicators · Flash photolysis · Fluorescence transients · DM-nitrophen · Kinetic modeling

A.L. Escobar · A.M. Kim · F. Cifuentes · J.L. Vergara (✉)
Department of Physiology, UCLA School of Medicine,
Los Angeles, CA 90024, USA

A.L. Escobar
Centro de Biofisica y Bioquimica,
Instituto Venezolano de Investigaciones Cientificas,
Altos de Pipe, Venezuela

P. Velez · M. Fill
Department of Physiology, Loyola University Chicago,
Maywood, IL 60153, USA

Introduction

The "caged Ca^{2+}" chelators Nitr-5 and DM-nitrophen (DM-n) [1, 20] have been increasingly used as tools to investigate the role of Ca^{2+} in the regulation of various biological processes ([7, 23, 24, 31]; for reviews see [18, 39, 40]). The photolysis of these compounds by ultraviolet (UV) light results in rapid increases in Ca^{2+} concentration ([Ca^{2+}]) that can be used to drive Ca^{2+}-dependent physiological processes. DM-n is particularly effective at releasing massive amounts of Ca^{2+} ions upon UV flash photolysis and thus, in spite of Mg^{2+}-binding limitations [9], has been widely used to investigate Ca^{2+}signaling [18, 19, 39].

Flash photolysis of solutions containing DM-n in excess over the total [Ca^{2+}] (for example 10 mM DM-n and 2 mM Ca^{2+}) can produce very fast, large changes in the free [Ca^{2+}] a few milliseconds after a UV flash [39]. This transient change in the free [Ca^{2+}] is mainly due to the rapid release of Ca^{2+} from DM-n and the slower rebinding of Ca^{2+} to the free DM-n remaining in the test solution. If DM-n is the predominant buffer species, the time course of this transient will depend primarily on the free DM-n concentration and the association rate constant for Ca^{2+} binding to DM-n. Attempts to quantitate the kinetics of these Ca^{2+} transients have been only moderately successful due to technical limitations in Ca^{2+} detection methodology and a lack of Ca^{2+} indicators able to track these transients [11, 35]. Until recently [11], it was not possible to use fluorescent [Ca^{2+}] indicators to measure the kinetics of this "spike" with a sub-millisecond time resolution. There is a consensus in the literature that the release of Ca^{2+} by flash photolysis of DM-n leads to the creation of "Ca^{2+} spikes" [9, 11, 12, 22, 29, 35, 39]. However, the characteristics of these spikes and the dependence of their kinetic properties on the initial experimental conditions have not yet been well documented. This shortage of information has been the basis for debates over the interpretation of data obtained from DM-n experiments [15–17, 21, 22]. More importantly, it has significantly limited the use of flash photolysis tech-

niques in investigations of Ca^{2+} regulation of physiological processes in living cells.

In this paper, we describe an experimental setup optimized to deliver UV flashes and to record the fast fluorescence transients resulting from the photolysis of DM-n. We used this system to characterize the kinetic properties of several commonly used fluorescent Ca^{2+} indicators [11, 12, 14, 30] and found that the Ca^{2+} indicator CalciumOrange-5N (COr-5N) [5, 11, 12] is able to adequately track the kinetic properties of transients elicited by flash photolysis of DM-n. Finally, we present a model that incorporates the kinetic parameters of DM-n and the Ca^{2+} dyes to describe the main features of the experimental data.

Materials and methods

Optical setup

A schematic diagram of the experimental setup is shown in Fig. 1A. It is a modification of the confocal spot detection system described previously [10] with an additional fiber optic to deliver flashes of UV light to droplets of dye-containing solutions in the field of view of the inverted fluorescence microscope. We used this optical setup to measure both the steady-state and kinetic Ca^{2+}-binding properties of several fluorescent Ca^{2+} indicators: Rhod-2, Fluo-3, CalciumGreen-2 (CGr-2), CalciumGreen-5N (CGr-5N) and COr-5N (Molecular Probes, Eugene, Ore., USA). The kinetic properties of the dyes were studied in response to rapid changes in $[Ca^{2+}]$ generated by flash photolysis of caged Ca^{2+} (DM-n tetrasodium salt; Calbiochem, La Jolla, Calif., USA).

The primary source for epifluorescence illumination was supplied by a multiline Argon laser (514 nm, 1 Watt; Model 95, Lexel, Freemont, Calif., USA). The laser beam was spatially filtered with a Gaussian filter (15 μm diameter pinhole) and then focused on the epifluorescence illumination port of an inverted microscope (Model IM, Zeiss, Oberkochen, Germany). A 20x objective (Fluo20, NA 0.75, Nikon, Japan) was used to form the pinhole image (illumination spot) and to collect fluorescence. The effective illumination spot measured 6 μm in diameter and was centered with respect to the fiber optic used to deliver UV pulses as shown in Fig. 1B. The excitation and barrier filters of a standard epifluorescence cube (FT-510; Zeiss) were removed so that only the dichroic mirror with a central wavelength of 510 nm was used. The barrier filter was replaced by long-pass colored glass filters (Oriel, Stratford, Conn., USA) with cut-on wavelengths at 570 nm for Rhod-2 and COr-5N, and at 530 nm for Fluo-3, CGr-2 and CGr-5N.

UV flash delivery

Flashes of UV light were generated by a frequency-doubled ruby laser (Lumonics, UK) and guided through a cladded fused-silica fiber optic (diameter 200 μm). The fiber optic was micropositioned with a hydraulic manipulator (Model OM3, Narishige, Japan) to lie close to the coverslip that constitutes the bottom of the experimental chamber (see Fig. 1A, B). Figure 1B shows the field of illumination with UV light by flashes delivered through the fiber optic. The fluorescence image (in Fig. 1B) was recorded with a thermoelectrically cooled charged coupled device (CCD) camera (Model MCD220, SpectraSource, Calif., USA) in a solution of rhodamine-G dye (Sigma, St. Louis, Mo., USA). The laser unit was able to generate UV light (340 nm) pulses of 50 ns duration at a maximal energy of 280 mJ. The energy of each UV flash was measured by a peak detection circuit located in the laser head whose output was acquired simultaneously with the fluorescence traces and calibrated with a digital bolometer (Model 36-5002T2, Scientech, Boulder, Colo., USA). The flash energies used in the present experiments ranged between 25 and 3000 μJ.

Fluorescence recording and elimination of flash artifact

The fluorescent light emitted by the Ca^{2+} dyes at the illumination spot was detected by an ultra low capacitance PIN photodiode with a square detection surface of 0.04 mm^2 (HR-008, United Detector Technologies, Culver City, Calif., USA) connected to an integrating headstage of a patch-clamp amplifier (Axopatch 200A, Axon Instruments, Foster City, Calif., USA). The depth of field of the confocal spot detection system with the PIN photodiode was estimated from confocal epifluorescence theory [37] to be approximately 6 μm. The gain and bandwidth of the patch-clamp amplifier, and the sampling rate of the data acquisition system (Axolab-1, Axon Instruments) were matched to the kinetic properties of the individual dyes to optimize the signal-to-noise ratio of the fluorescence traces as detailed in Table 1.

Although all the Ca^{2+} indicators investigated in this report are excited in the visible range of the light spectrum, far away from the UV wavelength used to photolyze DM-n, the high energy of the laser flash was able to generate enough fluorescence and light scattering in the dye-containing solution to overwhelm the highly sensitive recording system in the integrating mode of the patch-clamp. Trace A in Fig. 2 shows the large "flash artifact," detected by the photodiode during the UV flash, in the absence of epi-illumination. Trace B shows a fluorescence record in which the UV flash was delivered in the presence of epi-illumination, but without resetting the photodiode, to illustrate the relative magnitude of the flash artifact with respect to the increase in dye′s fluorescence following the photolysis of DM-n. Thus, the early phase of the flash-induced Ca^{2+} transient cannot be properly resolved due to the persistent saturation (for about 300 μs) of the photodetection system after the delivery of the UV flash. To prevent this saturation, the gain of the patch-clamp amplifier was set close to zero, by short-circuiting the integrating capacitor for 50 μs, while the UV flash was delivered. Trace C shows a fluorescence record obtained using the resetting

Fig. 1 **A** Schematic diagram of the experimental setup used to record fast fluorescence transients induced by flash photolysis of DM-nitrophen (*DM-n*). The basic optical components areμ an inverted microscope equipped with a standard epifluorescence port; an Argon laser which provides the high-intensity monochromatic light used to excite fluorescent dyes; a spatial filter which, in combination with the objective, focuses the beam into a spot in the preparation; and a photodiode centered on the spot that records the fluorescent light emitted by the dye in the experimental solutions. A small volume of solution is placed on a coverslip at the bottom of the experimental chamber that lies on the stage of the microscope. One end of the fiber optic receives the focused UV light from the frequency-doubled Ruby laser; the other end is introduced into the dye-containing solution and, with the aid of a micromanipulator, is placed very close to the Argon laser illumination spot. The PIN photodiode detector is placed exactly at the focal plane of the microscope and is centered at the point of maximal fluorescence emitted by the dye in solution. The fluorescence intensity is converted to current with a high-gain-patch-clamp amplifier and sampled by an analog-to-digital (A/D) converter interfaced with a 386/25 PC-compatible computer (*CPU no. 1*). This computer also triggers the UV flash and controls the gain of the patch-clamp amplifier through a digital interface (D/A) under program control. A Peltier-cooled CCD camera was used to image the field of illumination of the flash delivery system (see below). **B** Microscopy image of the illumination intensity profile by the UV fiber optic. Eight consecutive flashes of UV light (approximately 300 μJ/flash) were delivered to a solution containing 1 mM Rhodamine-G (Molecular Probes, Eugene, Ore., USA). It can be observed that although the excitation spectrum of this dye is shifted about 160 nm with respect to the 350 nm of the UV flash, the flash intensity was able to excite the chromophore and give enough fluorescent light to be detected as an image by the cooled CCD camera. The image shows the intensity distribution in a arbitrary linear intensity scale of 256 gray levels. The position of the spot of confocal detection (shown with a *circle*) was selected at sites where the intensity of UV excitation was almost maximal

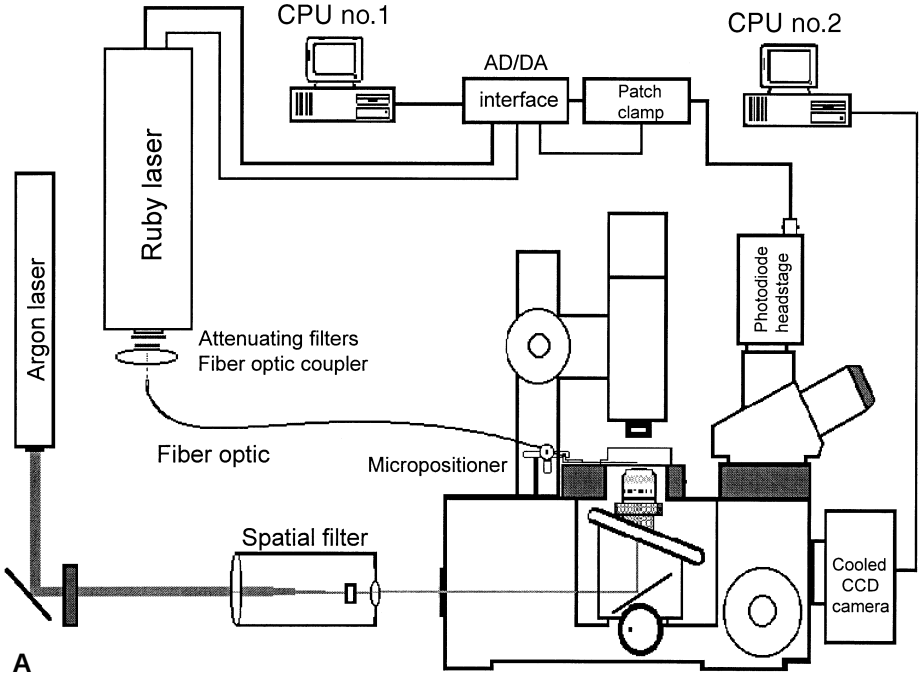

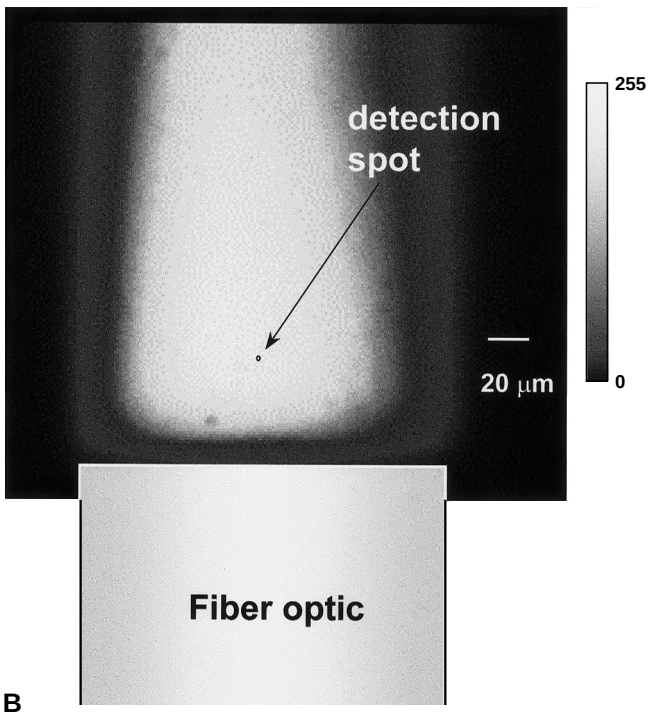

procedure. Note that in trace C the early rising phase of the dye response can now be clearly resolved in the absence of recording system saturation. The resetting procedure described above allowed recording of fluorescence transients with undistorted time courses within 10 μs after the delivery of UV flashes.

Dye bleaching

The fluorescence intensity of the dyes used in this report show the typical decay due to bleaching by the excitation light of the laser and, to a lesser extent, by the UV light used for flash photolysis. The time constant and magnitude of this decay depended on the intensity of the excitatory light, the degree of dye saturation and, most importantly, the dye used. To assess the influence of bleaching on the time course of the Ca^{2+}-dependent fluorescence transients, the maximal rate of bleaching of each dye (at saturating $[Ca^{2+}]$ and maximal excitation intensity) was determined with two parameters: maximal change in fluorescence, $\Delta_{b\text{-}max}$ (in % fluorescence), and minimal time constant of decay, $\tau_{b\text{-}min}$ (in ms). CGr-2 ($\Delta_{b\text{-}max}$ = 50%; $\tau_{b\text{-}min}$ = 6 ms) and, to a lesser extent, Fluo-3 ($\Delta_{b\text{-}}$

Table 1 Gain and data acquisition parameters. *CGr-2* CalciumGreen-2, *CGr-5N* CalciumGreen-5N, *COr-5N* CalciumOrange-5N)

Dye	Patch-clamp gain (mV/pA)	Bandwidth: Bessel 4-pole (kHz)	Sampling rate (μs/point)	Flash energy (μJoules)
Fluo-3	50	5	50	25–250
Rhod-2	50	5	50	25–250
CGr-2	50	5	50	25–250
CGr-5N	50	5	50	25–250
COr-5N	200	10–20	6	250-3000

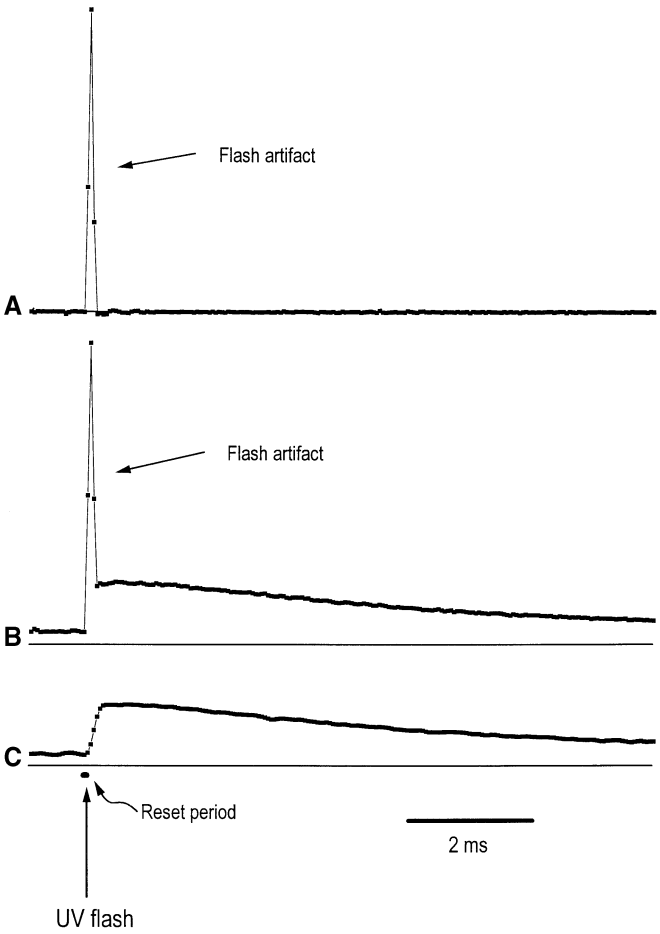

Fig. 2A, B Detection of fluorescence transients and elimination of UV flash artifact. **A** Light spike detected by the photodiode in response to the high-intensity illumination of the UV flash. In this case the solution was not epi-illuminated but the dichroic mirror and barrier filter were in place. **B** Fluorescence transient associated with the photolysis of DM-n plus UV flash artifact. The solution droplet containing DM-n and CaOr-5N with was epi-illuminated with the argon laser. **C** The same conditions as in **B**, but with the integrating capacitor of the patch-clamp amplifier head stage reset during the high energy UV illumination

$_{max}$ = 30%; $\tau_{b\text{-}min}$ = 16 ms) were the only dyes for which bleaching potentially affected the kinetic parameters reported below. The rest of the dyes showed less than 5% maximal bleaching within the longest acquisition (up to 2 s) period tested. The experimental traces shown in this paper were not corrected for bleaching, but the values of the kinetic rate constants were obtained from corrected records. To minimize the influence of bleaching in steady-sate calibrations, fluorescence data were obtained rapidly (within 1 ms) after opening of an electronic shutter controlling the laser epi-illumination.

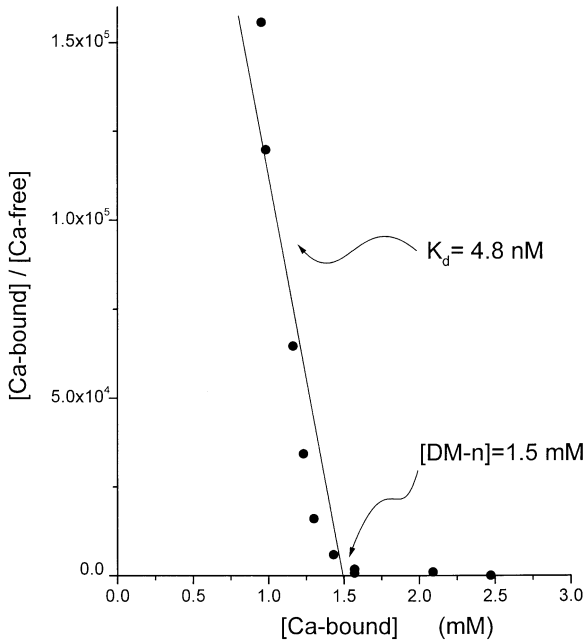

Fig. 3 Equilibrium properties of DM-n. Scatchard plot of the titration of a typical solution containing a nominal DM-n concentration of 2 mM. A Ca^{2+} electrode was utilized to record the free [Ca^{2+}] ([*Ca-free*]); [Ca-bound] was calculated as the difference between total added Ca^{2+} and the free [Ca^{2+}]. The linear regression fitted to the data (*solid line*; R = 0.98) predicts that the total [DM-n] (X-axis intercept) is 1.5 mM (instead of 2 mM) and that K_{DM} is 4.8 nM (reciprocal of slope). For details, see Bers [3] and DiPolo et al. [6]

Equilibrium properties of DM-n

The free [Ca^{2+}] was measured with custom-made Ca^{2+} electrodes [2, 6, 32] previously calibrated with pCa (–$\log_{10}$[Ca^{2+}]) standard solutions (Calbuff-1, WPI, New Haven, Conn., USA). Only those electrodes that showed linear behavior in the pCa range of from 2 to 8 were used.

The equilibrium dissociation constant (K_d) of DM-n and total concentration of DM-n in the experimental solutions were calculated from Scatchard plots of the titration data, according to the procedures described elsewhere [3, 6], as illustrated for a typical solution in Fig. 3. The average value of K_d for DM-n obtained from pooled data was 4.8 ± 0.8 × 10^{-9} M (mean ± SD; n = 4). The measured concentration of buffer was 73 ± 4 % (mean ± SD; n = 4) of that calculated from the manufacturer′s data. The concentrations of DM-n in the experiments were corrected by this factor.

Equilibrium properties of fluorescent Ca^{2+} indicators

The Ca^{2+}-binding properties of the fluorescent indicators were measured using two procedures:

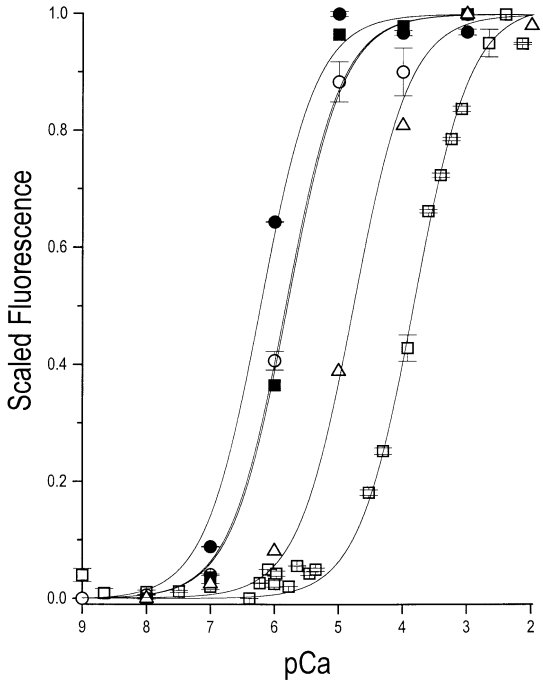

Fig. 4 Normalized saturation curves for the Ca^{2+} indicators. Fluo-3 (*solid circles*), Rhod-2 (*open circles*), CGr-2 (*solid squares*), CGr-5N (*open triangles*) and COr-5N (*open squares*). The calibrations were made as described in Materials and methods and were done in the absence of DM-n. The steady-state values for dissociation constants (K_d) and maximum change in fluorescence $(\Delta F/F)_{max}$ are included in Table 2

Method A: dyes dissolved in Ca^{2+} standards

First, 100 μM of the Ca^{2+}-sensitive dye was added to pCa standard solutions (pCa ranging from 9 to 2, 100 mM ionic strength, CALBUF-1, WPI; see [2]). Aliquots (5 μl) of these solutions were placed in the experimental chamber and their fluorescence was measured.

Method B: dyes dissolved in solutions standardized with Ca^{2+} electrodes

Solutions containing 100 mM KCl, various concentrations of DM-n, 10 mM 3-(*N*-morpholino)propanesulfonate, K^+ salt (MOPS-K), pH 7.0, and 100 μM of the Ca^{2+}-sensitive dyes were titrated (with $CaCl_2$) to set pCa values ranging from 9 to 2.

Unless otherwise stated, fluorescence data will be expressed throughout this manuscript in terms of normalized fluorescence ($\Delta\overline{F}$) defined as:

$$\Delta\overline{F} = \frac{F - F_{min}}{F_{max} - F_{min}} \quad (1)$$

where F is the measured fluorescence, F_{max} is the maximum fluorescence at saturating $[Ca^{2+}]$, and F_{min} is the minimum (maximally quenched) fluorescence at the lowest $[Ca^{2+}]$ tested (pCa 9). Figure 4 illustrates the equilibrium Ca^{2+}-binding properties of Fluo-3, Rhod-2, Cgr-2, CGr -5N, and COr-5N, by comparing their normalized fluorescence as a function of the free $[Ca^{2+}]$ of standard solutions (see above). The K_d valuesof these dyes were obtained by fitting the normalized data to the dye saturation curve

$$\Delta\overline{F} = \frac{1}{1 + \frac{K_d}{[Ca^{2+}]}} \quad (2)$$

Table 2 contains K_d values, thus determined, for each of the indicators under different experimental conditions. In addition, Table 2 includes (column 5) experimental values for the maximal fluorescence ratios $(\Delta F/F)_{max}$, defined as:

$$\left(\frac{\Delta\overline{F}}{\overline{F}}\right)_{max} = \frac{F_{max} - F_{min}}{F_{min}} \quad (3)$$

It should be noted that in Table 2 that different properties were observed for different batches of the same dye. For example, in 1994 (purchased after May) the K_d of CGr-5N changed from 36 μM to 17 μM, and in 1995 (after January) the K_d of COr-5N changed from 74 μM to 180 μM. Affinity changes were not due to variability in the measurements, as the latter were highly reproducible and strictly dependent on the dye lot.

Effects of DM-n on the steady-state properties of the Ca^{2+} indicators

Steady-state calibrations for the Ca^{2+} indicators were made in presence of 1.4–7 mM DM-n. Table 2 shows that DM-n does not have important effects on the apparent K_d and $(\Delta F/F)_{max}$ of Fluo-3, CGr-2, and COr-5N. The only dye moderately affected by DM-n was Rhod-2, which showed 50% change in affinity and a quenching effect on $(\Delta F/F)_{max}$ by a factor of 3.

Flash photolysis and fluorescence transients

Solutions containing 100 mM KCl, 1-10 mM DM-n, 10-100 μM of selected Ca^{2+}-sensitive dyes, and with pCa adjusted to set values, were placed in the experimental chamber for flash photolysis experiments. Unless otherwise stated, the fluorescence transients

Table 2 Equilibrium properties of fluorescence Ca^{2+} indicators

Dye	Calibration procedure[a]	[DM-nitrophen] (mM)	K_d (μM) mean±SD	$(\Delta F/F)_{max}$ mean±SD	Number of measurements
Fluo-3	Method A	–	0.6 ±0.1	30.9 ±0.8	3
Fluo-3	Method B	1.4	0.6 ±0.1	31.3 ±0.9	2
Fluo-3	Method B	7	0.74±0.2	28.7 ±1.2	2
Rhod-2	Method A	–	1.3 ±0.2	175.5 ±16.8	4
Rhod-2	Method B	7	1.87	66.8	1
CGr-2	Method A	–	1.58	32.9	1
CGr-2	Method B	7	1.94	22.2	
CGr-5N	Method A	–	17 ±1.8	11.4 ±0.2	2
CGr-5N[b]	Method A	–	36 ±10.7	14.3 ±1.1	3
COr-5N[c]	Method A	–	74 ±11.9	2.7 ±0.2	5
COr-5N	Methods A,B	–	180 ±9.9	2.5 ±0.2	13
COr-5N	Method B	1.4	196 ±5.2	2.2 ±0.1	2
COr-5N	Method B	7	192 ±4.5	2.8 ±0.1	2

[a] See Materials and methods
[b] Measurements before 5/1/94, the K_d is significantly different to that of earlier batches ($P<0.005$)
[c] Measurements before 1/1/95; the K_d is significantly different to that of later batches ($P<0.005$ see text)

observed are shown as normalized fluorescence changes ($\Delta\bar{F}$), as defined in Eq. 1, where F is the fluorescence acquired in every record as a function of time, F_{min} is the basal fluorescence recorded at very high pCa, and F_{max} is the fluorescence recorded at saturating [Ca^{2+}]. In practice, most of the experiments were performed in solutions with pCa values of ≈ 9, where the F_{rest} values, or the resting value of fluorescence before delivery of the flash (see Fig. 2) was always very close to F_{min}. Therefore, most cases the $\Delta\bar{F}$ traces have an initial baseline very close to zero and are normalized from 0 to 1. The advantage of this scaling method over the popular way of expressing fluorescence transients in terms of $\Delta F/F$, defined as $(F–F_{rest})/F_{rest}$ [36], is that the results obtained with different dyes are readily comparable. Moreover, for a total concentration $[D]_T$ of a dye that increases fluorescence emission upon binding Ca^{2+}, $\Delta\bar{F}$ is identical to the fraction of total indicator bound to Ca^{2+}:

$$\Delta\bar{F} = \frac{[\mathrm{CaD}]}{[D]_T} \tag{4}$$

Therefore, experimental records expressed as $\Delta\bar{F}$ can be readily compared with model predictions normalized accordingly. In addition, Table 3 contains the dye parameters necessary to transform scaled $\Delta\bar{F}$ fluorescence traces into $\Delta F/F$, which will allow the extension of these comparisons to data obtained under other experimental conditions.

Experiments were performed at 18°C, and results are presented as means ± SD of n observations. Statistical significance was assessed using an independent Student's t-test.

Results

Photolysis of DM-n generates very fast Ca^{2+} spikes

It has already been demonstrated that the Ca^{2+} indicator COr-5N has a low affinity for Ca^{2+} and is able to track rapid changes in [Ca^{2+}] resulting from flash photolysis of DM-n [11, 12]. Figure 5A shows a fluorescence "spike" detected by 100 μM COr-5N in response to flash photolysis of a solution containing 7 mM DM-n and a pCa of 9. It can be observed that the falling phase of the $\Delta\bar{F}$ signal is closely approximated by a simple exponential decay process with a time constant of 148 μs (continuous trace, Fig. 5A).

Ca^{2+} spikes as tools for evaluating kinetic rate constants of fluorescent indicators

Ca^{2+}–dye interactions yielding fluorescence signals such as the one reported in Fig. 5A can be readily analyzed given the following conditions: (1) the indicator follows the kinetic scheme of a simple bimolecular binding reaction; (2) photolysis of DM-n releases and rebinds Ca^{2+} with much faster kinetics than the Ca^{2+}–dye equilibration process, and thus generates a quasi-delta function spike of free [Ca^{2+}]; (3) the concentration of free indicator is much lower than the concentration of free DM-n so that the dye does not compete with DM-n in generating the [Ca^{2+}] spike's kinetics; and (4) the concentration of free indicator is in excess of that of the Ca^{2+}–dye complex. Under these conditions, the predicted time course of the fluorescence signal is given by the equation:

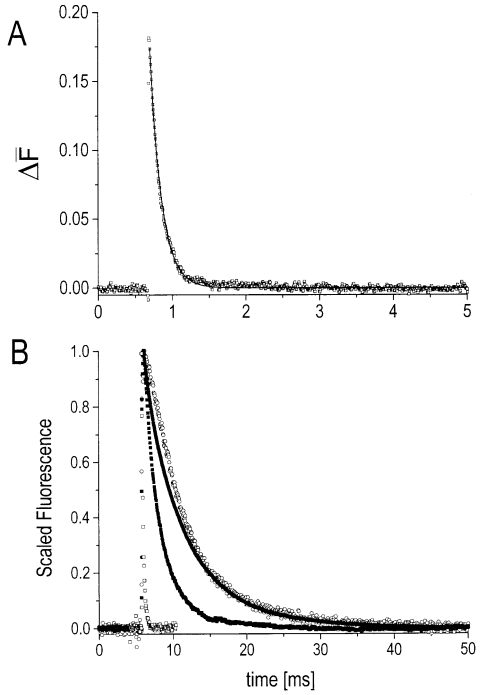

Fig. 5A, B Fluorescence transients elicited by flash photolysis of DM-n at pCa values close to 9. **A** COr-5N fluorescence (*open squares*) in response to Ca^{2+} released by photolysis of DM-n at a resting $[Ca^{2+}]_{t=0}$ = 3 nM. The time constant of decay of the fitted exponential (*solid line*) is 150 μs in this case. **B** Normalized fluorescence responses of different Ca^{2+} indicators: Fluo-3 (*solid circles*), Rhod-2 (*open circles*), CGr-2 (*solid squares*) and COr-5N (*open squares*). The respective decay time constants are included in Table 3

$$\Delta\bar{F}(t) = k_{on}\cdot[Ca^{2+}]_{peak}\cdot\tau\cdot\exp(-t\cdot k_{off}) \tag{5}$$

where $[Ca^{2+}]_{peak}\cdot\tau$ is the time integral of the [Ca^{2+}] spike, k_{on} and k_{off} are the association and dissociation rate constants of the dye, respectively, and is the normalized fluorescence change. A derivation of this equation is presented in Appendix A.

Figure 5B shows scaled experimental traces obtained with four different Ca^{2+} indicators in response to DM-n Ca^{2+} spikes at a pCa of 9. It can be observed that the decay time constants of fluorescence records obtained with higher affinity dyes, such as Fluo-3, Rhod-2 and CGr-2, were at least ten times longer that the one obtained with COr-5N. The actual values of these time constants are listed as τ_{off} in Table 3.

A prediction of Eq. 5 is that the time constant of decay of traces should be independent of the amplitude of the [Ca^{2+}] spike. We tested the validity of this prediction using a wide range of UV flash energies to generate spikes of different amplitudes with DM-n at pCa 9. The results of these experiments are illustrated in Fig. 6, where it can be observed that while the decay constants (τ values) of single exponentials fitted to fluorescence differ for the individual indicators, they are independent of the flash energy. Therefore, given the conditions presented with Eq. 5, the dissociation rate constants (k_{off})

Table 3 Kinetic rate constants of Ca^{2+}indicators. The equilibrium dissociation constants for each dye were the same as those presented in Table 2 in the presence of 7.2 mM DM-n. The decay time constants (τ_{off}) for each dye were obtained by fitting single exponential functions to at least 20 traces, similar to those shown in Fig. 5B. The dissociation rate constants k_{off} were calculated as the reciprocal of τ_{off}. The association rate constants (k_{on}) were obtained as k_{off}/K_d

Dye	K_d (μM) (mean±SD)	τ_{off} (ms) (mean±SD)	k_{off} (ms^{-1}) (mean±SD)	k_{on} ($\mu M^{-1}\ ms^{-1}$) (mean±SD)
Fluo-3	0.74±0.2	5.72 ±0.09	0.175±0.002	0.236±0.004
Rhod-2	1.87	7.85 ±0.15	0.130±0.002	0.069±0.003
CGr-2	1.94	2.09 ±0.03	0.479±0.007	0.246±0.007
COr-5N	192.4 ±4.5	0.155±0.013	6.51 ±0.118	0.033±0.006

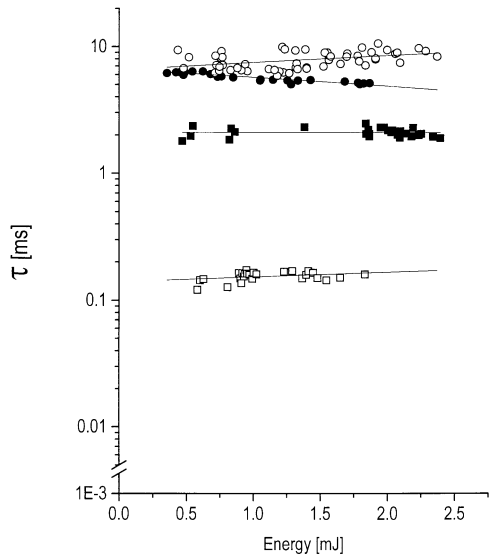

Fig. 6 Flash energy dependence of decay time constants of several indicators. The time constants of decay of fluorescence transients for Fluo-3 (*solid circles*), Rhod-2 (*open circles*), CGr-2 (*solid squares*) and COr-5N (*open squares*) are plotted semi-logarithmically as a function of flash energy. Linear fits to each set of data points are shown (*solid lines*) to illustrate that, for each dye, τ remains relatively constant over the entire range of energies tested. The mean values for the time constants are shown in Table 3. Experiments were performed at free Ca^{2+} concentrations close to pCa 9

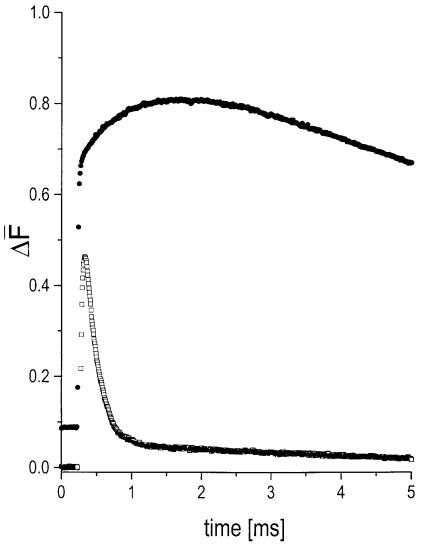

Fig. 7 Detection of flash photolysis Ca^{2+} release with a fast indicator (COr-5N, *open squares*) compared with a slower indicator (Fluo-3, *solid circles*). The resting free [Ca^{2+}] was close to pCa 7. The dye concentration in both cases was 100 μM and the total concentration of DM-n was 7.2 mM. The energy of the flash was 820 μJ for both transients

for the individual Ca^{2+}–dye reactions can be calculated as the inverse of the decay time constants of the fluorescence spikes obtained with DM-n at pCa 9. Values of k_{off} thus obtained are tabulated in Table 3. Furthermore, the last column of this table contains predicted values for the association rate constant (k_{on}) of each dye, calculated from the ratio of k_{off} and the equilibrium dissociation constant (K_d).

Time course of the fluorescence signals at pCa 7

The experimental data obtained in DM-n flash photolysis experiments at pCa 9 are adequately predicted by Eq. 5. This suggests that the [Ca^{2+}] spikes generated under these conditions are very fast with respect to the dyes′ kinetic properties; hence, the time course of the fluorescence transients should primarly reflect the characteristics of the indicators rather than those of the releasing agent (DM-n).

Since DM-n and the fluorescent indicators mentioned above are widely used in biological tissues, the issue of their kinetic behavior at physiological free [Ca^{2+}] is relevant. The law of mass action and previous observations about the physical chemistry of DM-n predict that the properties of Ca^{2+} transients elicited by flash photolysis of DM-n should depend strongly on its resting fractional complexation with Ca^{2+} [29, 39]. To investigate this, we used experimental conditions similar to those in Fig. 5 but selected a resting free Ca^{2+} level of about 100 nM (pCa 7; see [28]). The results from these experiments are shown in Fig. 7. The COr-5N record (open squares) shows an early “spike” in fluorescence which decays rapidly to a sustained level above baseline, suggestive of a rapid increase in free [Ca^{2+}] followed by rebinding of Ca^{2+} by a diminished fraction of DM-n. In contrast, the Fluo-3 transient (closed circles) shows a significantly

broader time course, indicating that this dye is unable to track the true time course of the changes in free [Ca^{2+}] [11].

COr-5N fluorescence transients observed with UV flashes of approximately the same energy are larger at pCa 7 (Fig. 7, lower trace) than at pCa 9 (Fig. 5A). This marked increase in amplitude (2.6 times) is consistent with the liberation of more Ca^{2+} at pCa 7, where nearly 96% of DM-n is bound to Ca^{2+}, than at pCa 9, when only 18% is bound (see Fig. 3B, also [18, 19, 39]. Qualitatively, all the dyes reported transients with larger amplitudes at low pCa values than at high pCa values for similar UV energies (data not shown). However, an accurate quantitative analysis of the pCa dependence of the fluorescence transients requires a multi-factorial non-linear model as discussed below. It is also important to note that the COr-5N transient recorded at pCa 7 decays with a relaxation time constant of 181 ± 10 μs (n = 27), significantly slower (P<0.01) than the one measured with the same dye at pCa 9 (155 ± 13 μs, n = 26). Although this kinetic disparity is expected, since at pCa 7 there is less free DM-n to participate in the rebinding process [18, 19, 39], here, again, a quantitative model is necessary to delineate the interplay of the various parameters governing the non-equilibrium processes involved in these experiments.

A model for DM-n photolysis and its interaction with Ca^{2+} indicators

The assumptions proposed in the derivation of Eq. 5 are not necessarily valid at pCa values lower than 9. In these cases, photolysis of DM-n may generate changes in free [Ca^{2+}] with longer time courses than the postulated quasi-delta function at pCa 9. Moreover, because photolysis at lower pCa values releases more free Ca^{2+}, the concentration of free indicator may not necessarily be in excess with respect to the Ca^{2+}–dye complex. As such, the simplified theoretical framework developed in Appendix A neither provides an accurate representation of the experimental conditions of Ca^{2+} release by flash photolysis of DM-n over a wide range of pCa, nor correctly describes the Ca^{2+}–dye interactions able to predict the fluorescence traces recorded with several indicators.

To address these limitations, we developed a more robust kinetic model (Appendix B) which includes equations for the DM-n photolysis reaction and for the kinetics of Ca^{2+} complexation by a fluorescent indicator. Incorporated into the model is the fact that during the photolysis reaction, DM-n undergoes a transition between a high-affinity (measured K_d = 4.8 nM, see Materials and methods) and a low-affinity state ($K_d \approx$ 3 mM; [20]) within a $\tau_{photolysis}$ of approximately 20 μs [9, 20]. It will be demonstrated below that model predictions enable us to quantitatively assess the true kinetics of Ca^{2+} release, independent of the conditions required for Eq. 5.

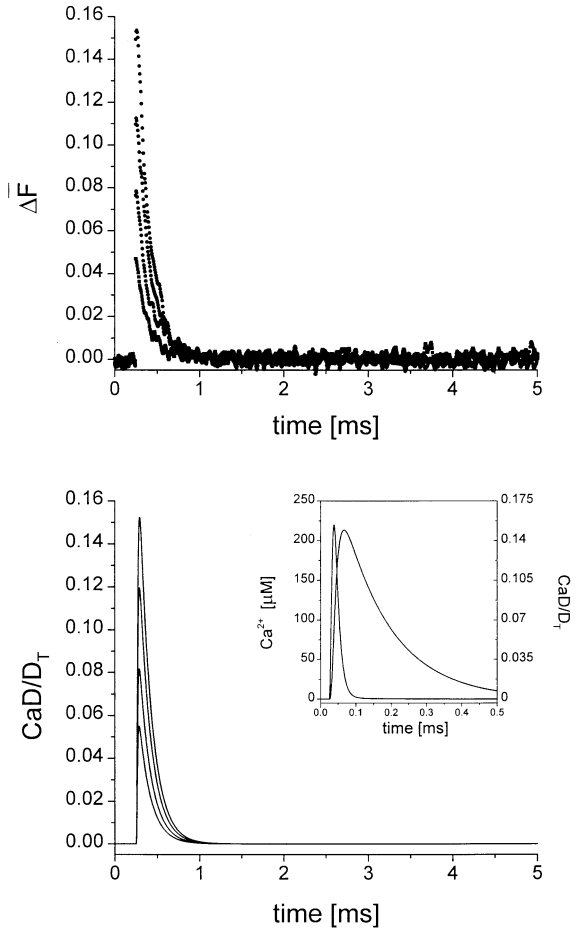

Fig. 8 Comparison between experimental COr-5N fluorescence transients obtained at a pCa of ≈9 and theoretical traces predicted by the model in Appendix B. **A** $\Delta\bar{F}$ transients (average of 4 records) in response to flash energies of 635, 904, 1319, and 1626 μJ. Larger amplitudes correspond to larger energies. Experimental solutions were as described in Method B (see Materials and methods), and contained 7.2 mM DM-n, 100 μM COr-5N, and $[Ca^{2+}]_{t=0}$ was adjusted to ≈4 nM. **B** CaD/D_T traces simulated with the following model parameters: $[D]_T$ = 100 μM, $[DM]_T$ = 7.2 mM, $[Ca^{2+}]_{t=0}$ = 3.5 nM, $k_{off\text{-}D}$ = 7.5 ms^{-1}, $k_{on\text{-}D}$ = 0.04 $\mu M^{-1}ms^{-1}$, K_{DM} = 4.4 nM, $k_{on\text{-}DM}$ = 0.03 $\mu M^{-1}ms^{-1}$, $k^*_{off\text{-}DM}$ = 75 ms^{-1}, $\tau_{photolysis}$ = 20 μs, t_{pulse} = 0.25 ms. In order of increasing CaD/D_T, α was 0.080, 0.115, 0.162 and 0.200 (see Appendix B for explanation of variables). *Inset:* predicted free Ca^{2+} spike superimposed on CaD/D_T trace for α=0.20. In this case, the flash pulse was delivered at t_{pulse} = 0.025 ms

Model predictions at high pCa values

Figure 8A shows normalized COr-5N fluorescence transients recorded in response to flash photolysis of a solution containing 7.2 mM DM-n, 100 μM of the indicator, and a pCa of 8.5, obtained by Method B. UV flash pulses were delivered with four different energies ranging between 0.65 and 1.62 mJ. Panel B in Fig. 8 shows the CaD/D_T traces obtained by integration of the differential equations in Appendix B. The parameter values adjusted to obtain the demonstrated good agreement between model predictions and experimental data notably include a dissociation rate constant for COr-5N

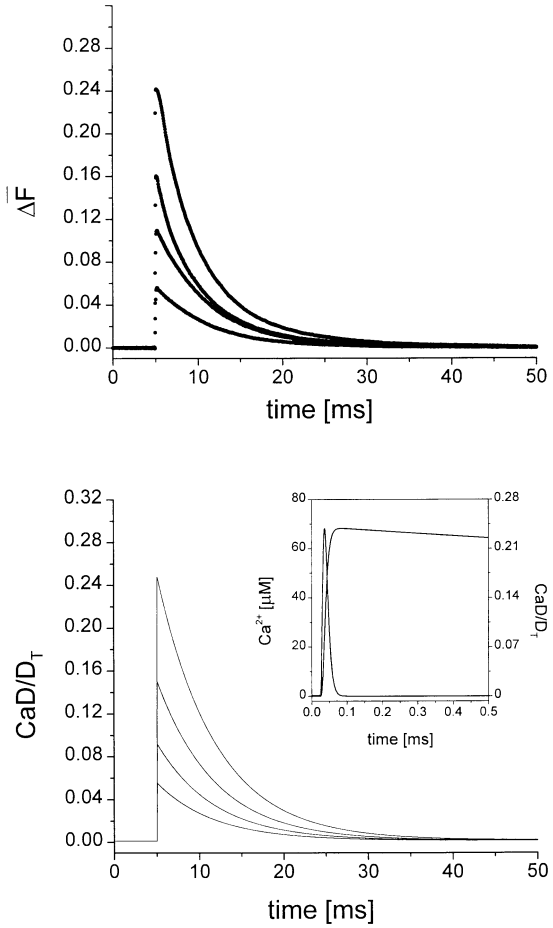

Fig. 9 Comparison between experimental Fluo-3 fluorescence transients at a pCa of ≈9 and model predictions. **A** $\Delta\bar{F}$ transients (average of 4 records) obtained with the same protocol as in Fig. 8A, but in a solution containing 100 μM Fluo-3 as the Ca^{2+} indicator. Flash energies were 425, 714, 1123, and 1814 μJ, corresponding to the records in order of increasing magnitude. **B** Model predictions for the following conditions: $[D]_T$ = 100 μM, $[DM]_T$ = 7.0 mM, $[Ca^{2+}]_{t=0}$ = 0.9 nM, $k_{off\text{-}D}$ = 0.16 ms^{-1}, $k_{on\text{-}D}$ = 0.22 $\mu M^{-1}ms^{-1}$, K_{DM} = 4.4 nM, $k_{on\text{-}DM}$ = 0.03 $\mu M^{-1}ms^{-1}$, and α was 0.005, 0.087, 0.138 and 0.220, in order of increasing CaD/D_T (see Appendix B). Other simulation parameters are identical to those in Fig. 8B. *Inset:* predicted free Ca^{2+} spike superimposed on CaD/D_T trace for α=0.220. Here again, the flash pulse was delivered at t_{pulse} = 0.025 ms

(7.5 ms^{-1}) similar to that determined with Eq. 5 (6.51 ms^{-1}, Table 3), and an association rate constant for DM-n (0.03 μM^{-1} ms^{-1}) consistent with that previously reported by the authors [11], but significantly faster than the 0.0015 $\mu M^{-1}ms^{-1}$ reported by Zucker [39]. The inset in Fig. 8B shows, on an expanded time scale, the time course of a typical COr-5N CaD/D_T trace superimposed on the predicted free $[Ca^{2+}]$ spike. It is important to note that while the free $[Ca^{2+}]$ spike is essentially over in about 100 μs (τ<15 μs), the COr-5N transient lingers above baseline beyond 500 μs, demonstrating that even this fast, low-affinity Ca^{2+} indicator is somewhat limited in its ability to track the kinetics and amplitude of the $[Ca^{2+}]$ spike.

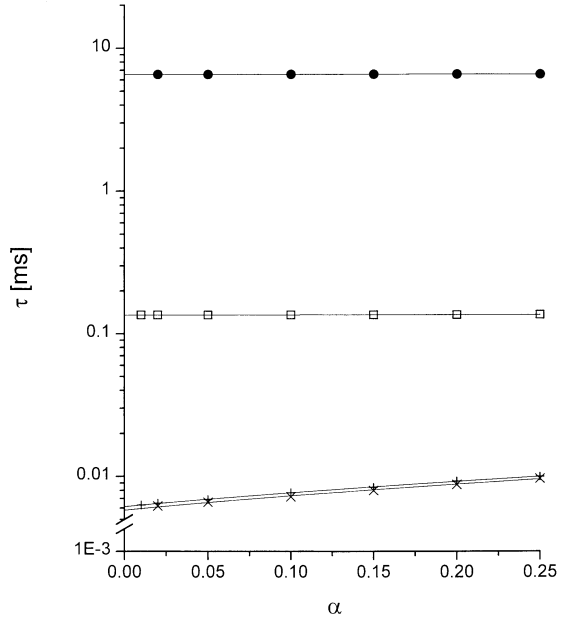

Fig. 10 Semi-logarithmic τ vs α plots of model predictions. Values for τ were obtained by fitting single exponentials to model simulations of CaD/D_T transients for Fluo-3 (*solid circles*) and COr-5N (*solid squares*); similarly, *open symbols* correspond to τ values fitted to the respective simulated free Ca^{2+} transients. The parameters for DM-n and the respective dyes were the same as those used in Figs. 8 and 9

Figure 9 shows results of a similar experiment using the slower, higher affinity Ca^{2+} indicator Fluo-3. In this case, the solution contained 7.2 mM DM-n, 100 μM Fluo-3, and had a pCa of 9. UV flashes (four energies, 0.42-1.81 mJ) were delivered and produced the experimental records shown in panel A. Note that the time scales for the Fluo-3 traces are 10 times slower than those for the COr-5N experiment (Fig. 8). After adjusting only the Ca^{2+}-sensitive dye kinetic parameters, the resting free $[Ca^{2+}]$, and the fraction of DM-n photolyzed (α), numerical integration of the model produces the traces shown in Fig. 9B, which again are in agreement with the experimental data. Note that the model's dissociation rate constant for Fluo-3 (0.16 ms^{-1}) compares well with that determined by Eq. 5 (≈0.18 ms^{-1}, Table 3). The inset of Fig. 9B shows both the waveform of the predicted free $[Ca^{2+}]$ and the time course of CaD/D_T for α = 0.22. In this time frame, it can be seen that the predicted free Ca^{2+} spike is over in less than 100 μs, but the Fluo-3 signal dwells at elevated levels that are far below dye saturation. This behavior exemplifies the limitations of a relatively high-affinity dye with a slow dissociation rate constant. It should also be noted, shown in the inset of Fig. 9B, that the amplitude of the predicted free Ca^{2+} spike is significantly smaller than the one in the inset of Fig. 8B (68 μM vs 220 μM), even though the photolyzed fraction was slightly larger in the former case (22% vs 20%). This result is due partially to the difference in the initial $[Ca^{2+}]$ between these model predictions (0.9 vs 3.5 nM), reflecting the influence of the resting free $[Ca^{2+}]$ on the amount

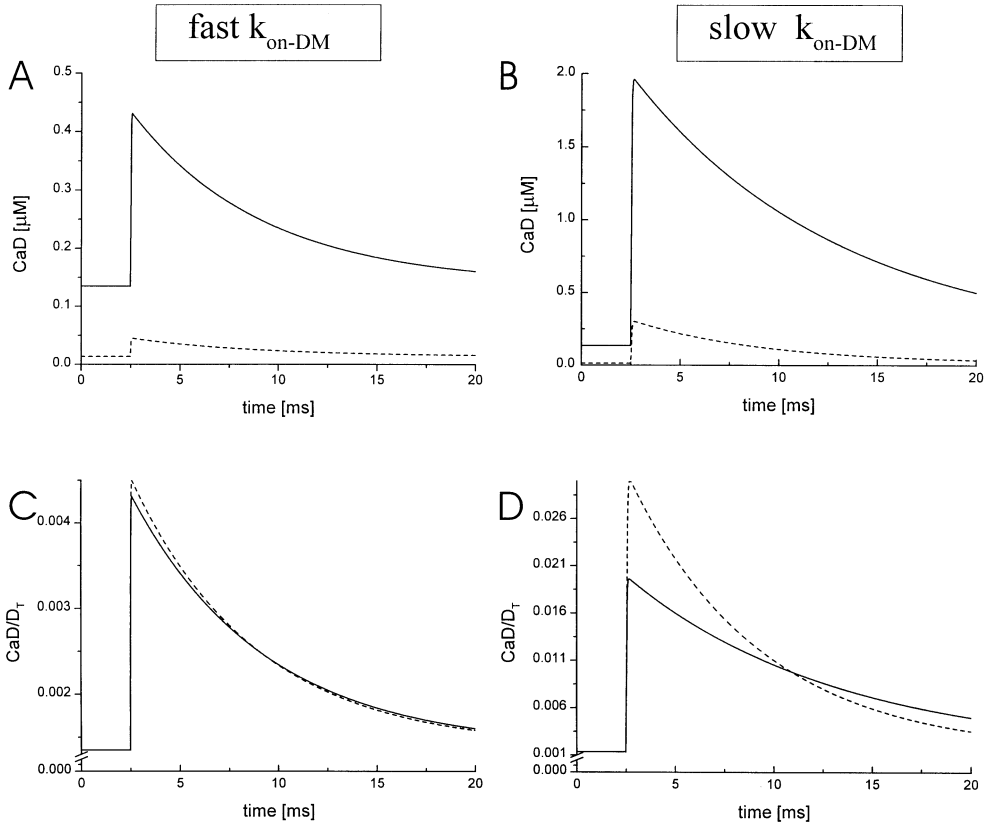

Fig. 11 Predicted time course of Fluo-3 fluorescence transients at two dye concentrations and two association rate constants for DM-n. **A** Simulations for the concentration of dye complexed with Ca^{2+} for the following parametersμ $[DM]_T$= 7.0 mM; $[Ca^{2+}]_{t=0}$ = 1 nM; $k_{off\text{-}D}$=160 ms^{-1}; equilibrium dissociation constants for the dye, K_D= 0.74 μM, and for DM-n, K_{DM}= 4 nM; $k_{on\text{-}DM}$= 0.03 $\mu M^{-1}ms^{-1}$; and α=0.0013. *Continuous trace* $[D]_T$= 100 μM; *dashed trace* $[D]_T$= 10 μM. **B** Same as **A**, but $k_{on\text{-}DM}$= 0.003 $\mu M^{-1}ms^{-1}$. **C** Same as **A**, but normalized by D_T. **D** Same as **B**, but normalized by D_T

of Ca–DM-n complex that is photolyzed, and also to the difference in $k_{on\text{-}D}$ values for COr-5N and Fluo-3.

It should be noted that free $[Ca^{2+}]$ spikes lasting for <100 μs, a common feature in Figs. 8B and 9B, are only attained with the selection of a very fast association rate constant for DM-n. Slower values of this rate constant predict longer free $[Ca^{2+}]$ spikes which, in turn, result in fluorescence transients inconsistent with the experimental records obtained with both dyes.

To further characterize the model's predictions, we fitted single exponentials to the falling phases of CaD/D_T traces simulated with the parameters described in Fig. 8 for COr-5N, and in Fig. 9 for Fluo-3. The corresponding time constants, τ, are plotted in Fig. 10 as a function of α. It can be seen that, for both dyes, the fitted decay time constants are independent of α, a finding which is consistent with the experimental results shown in Fig. 6. The quantitative accuracy of the model can be observed in the numerical consistency between the predicted (Fig. 10) and experimental (Fig. 6) τ values for both Fluo-3 and COr-5N. The lack of correlation between α and τ even at high values of α suggests that, at pCa 9, the photolysis-induced Ca^{2+} spikes occur on a substantially faster time scale than that of the Ca^{2+}–dye dissociation process. This concurs with the free Ca^{2+} time courses presented in the insets of Figs. 8 and 9; and supports the validity of the results calculated with Eq. 5 (Table 3), which assumes that the photolysis Ca^{2+} spike at pCa 9 resembles a delta function in time.

Association rate constant of DM-n

As mentioned above, the association rate constant of DM-n ($k_{on\text{-}DM}$) that best predicted our experimental data was approximately 20 times faster than that reported by Zucker [39]. Since this parameter value has important implications for the interpretation of results obtained in DM-n flash photolysis experiments using biological preparations [13, 23, 39], we chose to determine it in a more rigorous manner. Model simulations suggested to us that varying the dye concentration, while keeping all other parameters constant, could provide a sensitive procedure to quantitatively resolve the effects of $k_{on\text{-}DM}$ on the time course of fluorescence transients. Figure 11 illustrates this. Panel A shows model predictions for Fluo-3 transients using the $k_{on\text{-}DM}$ = 0.03 $\mu M^{-1}ms^{-1}$ as per Fig. 8 (see above) at 100 μM (continuous trace) and 10 μM (dashed trace) dye concentrations. Similarly, panel B shows an identical simulation, but with a tenfold slower $k_{on\text{-}DM}$ (0.003 $\mu M^{-1}ms^{-1}$). As expected, both a higher dye concentration and a slower $k_{on\text{-}DM}$ result in empirically larger transients. Normalized fluorescence simulations (CaD/D_T), which are analogous to experimental transients and allow the comparison of model predictions at different dye concentrations, are shown in panels C and D. Interestingly, the normalized fluorescence traces calculated for high and low dye concentrations are virtually identical when the faster $k_{on\text{-}DM}$ (panel C) is used, but are significantly different when the slower $k_{on\text{-}DM}$ (panel D) is used.

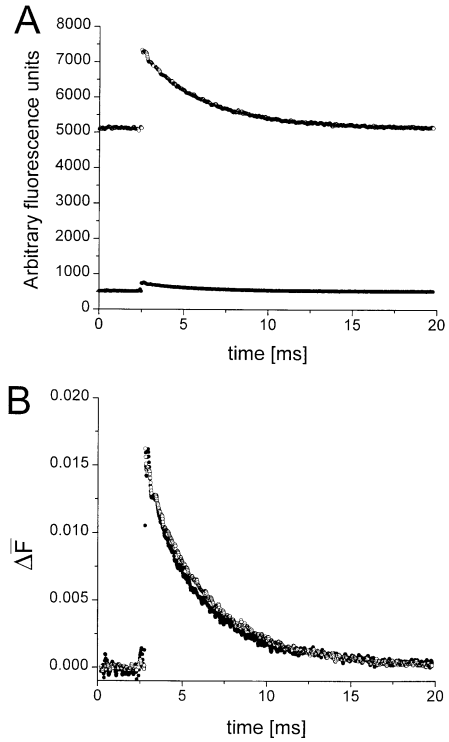

Fig. 12A, B Flash photolysis Ca^{2+} transients recorded at two different concentrations of Fluo-3. **A** Traces represent the average of 4 transients recorded in response to flashes of 80 μJ. *Upper trace* (*open circles*) recorded with 100 μM Fluo-3, *lower trace* (solid circles) measured with 10 μM Fluo-3. The difference in resting fluorescence reflects the difference in the dye concentration. **B** Same data as in **A**, but normalized as $\Delta\bar{F}$ (see Materials and methods)

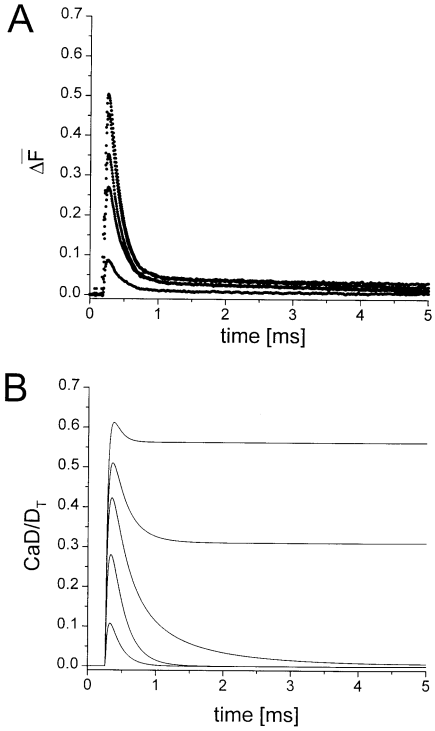

Fig. 13A, B Fluorescence transients at pCa ≈7 and corresponding theoretical traces predicted by the model shown in Appendix B. **A** Transients elicited by flashing a solution containing 7.2 mM DM-n and 100 μM COr-5N. The resting free Ca^{2+} was approximately 45 nM. Each *trace* represents the average of 4 records taken at flash energies of 147, 460, 708, 880, and 1110 μJ, respectively. **B** Simulated traces for the following conditions: $[D]_T$=100 μM, $[DM]_T$=7.2 mM, $[Ca^{2+}]_{t=0}$= 45 nM, $k_{off\text{-}D}$=7.5 ms^{-1}, K_D=187 μM, K_{DM}=4.8 nM, and $k_{on\text{-}DM}$=0.03 $\mu M^{-1}ms^{-1}$. In order of increasing CaD/D_T, α = 0.021, 0.056, 0.087, 0.108 and 0.136

To parallel these simulations experimentally, fluorescence records were obtained by flash photolysis of solutions containing 7 mM DM-n at pCa 9 in the presence of 100 μM and 10 μM Fluo-3, maintaining a constant flash energy. Data from a typical experiment are shown in Fig. 12. In agreement with the model simulations, raw fluorescence transients elicited at these dye concentrations are dissimilar. However, when the traces are normalized in units (panel B), they are nearly superimposable. This relationship, which was invariably preserved in many other trials (n>10), suggests that the effective $k_{on\text{-}DM}$ of DM-n is consistent with a 0.03 $\mu M^{-1}ms^{-1}$ value as stated above, but not with a tenfold slower value.

Flash energy dependence of fluorescence signalsμ experiments vs model

To further test the predictive fidelity of the model and its parameter values, we varied the energy of the UV flashes applied experimentally and compared these results with model predictions where the α values were varied accordingly. Fluorescence transients recorded in 7.2 mM DM-n, 100 μM COr-5N, and at a pCa of 7.4 are shown in Fig. 13A. Each of the five transients (flash energy = 0.17-1.1 mJ) shows a time course characterized by an early spike which decays to a plateau. The magnitude of both the spike and the plateau phases are directly dependent on the energy of the flash applied. Figure 13B shows the corresponding model predictions in which α was varied between 0.02 and 0.13. It can be observed that model and experimental traces concur at the two lower energies, but the model traces at the three higher energies progressively diverge from experimental data, particularly in the plateau phase.

Robust pH buffering strengthens agreement between model predictions and experimental data at lower pCa values

A factor that may underlie the discrepancies between model predictions and experimental data at higher energies shown in Fig. 13 is the occurrence of pCa-dependent pH changes. Because of the large proportion of DM-n complexed with Ca^{2+} at lower pCa values, photolyzing DM-n results in extremely large concentrations of free Ca^{2+} released at the higher flash energies. These, in turn, may promote a significant dynamic alteration of solution pH during the transient.

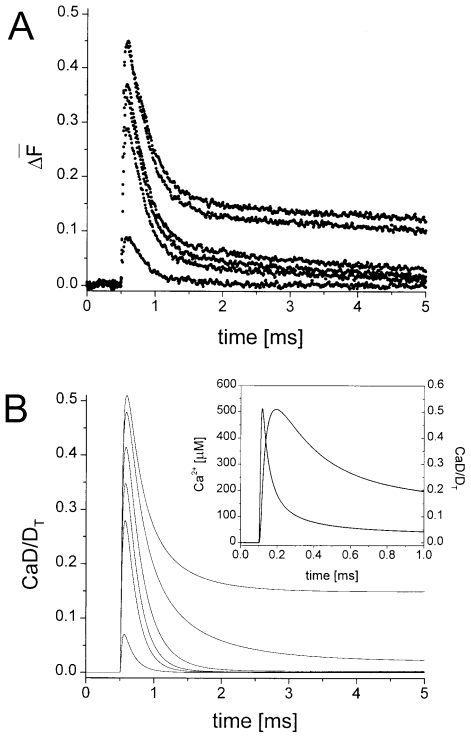

Fig. 14A, B Experimental fluorescence transients recorded from a highly pH buffered solution (pCa ≈7) and the corresponding theoretical traces predicted by the model shown in Appendix B for **A**. **A** Fluorescence transients obtained in a solution identical to that of Fig. 13, but with 110 mM K-MOPS at pH 7.0. Each *trace* represents the average of 4 records elicited by flashes of 136, 449, 666, 901, 1137, and 1258 µJ. Larger trace magnitudes correspond to larger energies. **B** Simulated traces for the same conditions as Fig. 13B, but with K_{DM}= 19 nM. In order of ascending trace magnitude, corresponding values for α were 0.02, 0.08, 0.10, 0.12, 0.14, and 0.15, respectively. *Inset:* expanded time course representation of the predicted free [Ca^{2+}] (α=0.15) and the corresponding fraction of dye complexed

To test for this effect, chloride in the solution described in Method B was completely replaced by the proton buffer MOPS (final concentration 110 mM MOPS-K). Scatchard plots for this solution predicted that the dissociation constant of DM-n shifted from 4.8 nM to 19 nM in the presence of 110 mM MOPS-K at pH 7 (data not shown).

Flash photolysis transients recorded in such a highly pH buffered solution are shown in Fig. 14A. In comparison with transients obtained in the less pH buffered solutions (Fig. 13A), the time constants for the decay of the fluorescence spike towards the plateau phase were slightly slower in this case. Interestingly, under these experimental conditions, the model accurately predicts the corresponding experimental traces over the entire range of energies tested (Fig. 14B vs Fig. 14A). It should be noted that in these model simulations, the effective dissociation constant of DM-n used was that derived from the Scatchard plot obtained for the high-MOPS solution.

The inset of Fig. 14 shows, on an expanded time scale, the predicted fluorescence trace in Fig. 14B at the highest energy (α = 0.15) and the corresponding predicted free [Ca^{2+}] time course. The "spike and plateau" time course is evident in the free [Ca^{2+}] trace, and is reflected in the predicted fluorescence trace. Notably, the free [Ca^{2+}] level during the spike rises to ≈500 µM, and visibly precedes the dye fluorescence peak (≈0.5 CaD/D_T). The plateau phase of the free Ca^{2+} trace "settles" to ≈50 µM within <1 ms, while the fluorescence plateau does not reach a steady-state within this time frame.

Discussion

We have developed a new methodology that allows localized detection of rapid fluorescence transients in response to laser flash photolysis of caged Ca^{2+}. We used this technique to quantitatively evaluate kinetic rate constants that characterize several commonly used Ca^{2+}-sensitive fluorescent indicators, and to resolve the kinetic intricacies of Ca^{2+} unbinding from, and rebinding to, DM-n.

Kinetic parameters of Ca^{2+} indicators obtained from "Ca^{2+} spikes" experiments

We began by establishing that photolysis of high concentrations of DM-n at high pCa values released very fast Ca^{2+} spikes (quasi-delta functions) which provided a simple means to evaluate the kinetic rate constants of Ca^{2+}-sensitive fluorescent dyes according to the mathematical framework in Appendix A. Specifically, single exponential fits to the decay phases of flash-induced fluorescence transients (Fig. 5) provided the effective dissociation rate constants (k_{off} values) of the dyes within the approximations of Eq. A7 (Appendix A; also Eq. 5). A critical issue in measuring these rate constants was the ability to discern the rising, as well as the falling, phases of the fluorescence transients in response to flash photolysis of DM-n. As demonstrated in Fig. 2 and as described in Materials and methods, we achieved this by blanking the headstage of the patch-clamp amplifier during the laser flash. The resulting experimental records were free of flash-induced contamination during the rising phase of fluorescence and hence amenable to quantitative comparison with theoretical predictions.

Under the same experimental conditions as those of the photolysis experiments, we completed the kinetic analysis by fitting saturation curves (Fig. 4) to determine the equilibrium properties [i.e., K_d, $(\Delta F/F)_{max}$; Table 2] of each dye tested. We did this in the presence of different concentrations of DM-n, as required for a thorough evaluation of the kinetic behavior of the Ca^{2+} indicators in the presence of the "caged" Ca^{2+}. In contrast to the proposals of Zucker [38] and Riecke and Schwartz [32], our results (Table 2) suggest that there is little interaction between DM-n and Ca^{2+} indicators. Our data do indicate, however, that the steady-state properties of commercially available indicators may differ in a batch-dependent

fashion, and that the actual experimentally obtained values for equilibrium dye parameters [K_d, $(\Delta F/F)_{max}$] can be significantly disparate from those published in manufacturers' specifications.

By measuring the k_{off} and the K_d of dyes, we calculated k_{on}. The resulting values for the kinetic parameters of the indicators (Table 3) demonstrate that the common assumption that k_{off} values are inversely proportional to dye affinities does not always apply. For example, in our hands, the higher affinity indicator Fluo-3 (K_d = 0.74 μM) had faster dissociation kinetics (k_{off} = 0.175 ms^{-1}) than the lower affinity indicator Rhod-2 (K_d = 1.87 μM; k_{off} = 0.130 ms^{-1}). However, the lowest affinity indicator tested (COr-5N, K_d = 192 μM) had the fastest k_{off} (6.51 ms^{-1}). On the other hand, the k_{on} values (Table 3), which were calculated from experimental measurements and not assumed a priori to be diffusion limited, varied for each indicator irrespective of its affinity. For example, Fluo-3 and CGr-2 showed very fast k_{on} values, approaching diffusion limitation, while the low-affinity dye COr-5N, whose kinetic behavior was significantly faster than that of Fluo-3 or CGr-2 (e.g. Figs. 5 and 7), actually had a k_{on} which was nearly an order of magnitude slower than that of the higher affinity dyes (see Table 3). It is interesting to note that the value of k_{on} for COr-5N reported here (3.3×10^7 $M^{-1}s^{-1}$) is also about an order of magnitude lower than the 3×10^8 $M^{-1}s^{-1}$ obtained by Ellis-Davies et al. [9]. In addition, their k_{off} value (1.26×10^4 s^{-1}) is not quite double the one reported here, compatible with a K_d (43 μM) about 5 times lower than our measurements. However, because of the equivocal description of the methods used by these authors to calculate their parameters (see pp 1009 and 1014 in [9]), the sources of these discrepancies are not obvious.

A concern we had with respect to the aforementioned measurements was whether they exclusively reflected the dyes' kinetic properties, or whether the "quasi-delta function" approximation of the flash photolysis Ca^{2+} spikes at high pCa values was inaccurate (i.e., the properties of DM-n were also reflected in the fluorescence measurements). As shown in Fig. 6, the time constants of decay (τ) of the fluorescence transients for every Ca^{2+} indicator tested at pCa 9 were independent of the UV flash energy, indicating that, under these conditions, the "quasi-delta function" approximation is accurate. Additional evidence ruling out spurious kinetic interactions between DM-n and the dyes came from experiments utilizing low (1.7 mM) and high (7.2 mM) concentrations of the caged compound at pCa 9. It was found that the τ values fitted under both conditions were virtually identical for every dye tested (results not shown).

In the case of Fluo-3, perhaps the most popular of the indicators tested, our values of k_{off} and k_{on} (175 s^{-1} and 2.4×10^8 $M^{-1}s^{-1}$, respectively) are both lower than the 424 s^{-1} and 9.8×10^8 $M^{-1}s^{-1}$ values reported by Lattanzio and Bartschat [25] using a stopped-flow method. At least part of the discrepancy may reside in the slight difference in pH at which the determinations were made (7 in our case and 7.4 in theirs). In fact, our K_d value (0.6 μM) is higher than their measurement at pH 7.4 (462 nM) but much lower than the one at pH 5.5 (5.4 μM). An additional discrepancy with the results from other laboratories [8, 25] is that we did not find evidence of the biexponential dissociation rates with Fluo-3.

Analysis of Ca^{2+} release by DM-n

We assessed DM-n–Ca^{2+} dye interactions with a mathematical model (Appendix B) that incorporates pertinent kinetic parameters and whose predictions are quantitatively consistent with experimental observations. It should be noted that flash energy, an experimental measurement that has heretofore been addressed only qualitatively in caged Ca^{2+} flash photolysis experiments [8, 39], is a key model parameter (α) for the adjustment of theoretical predictions of the experimental data. In addition, other critical model parameters include dissociation rate constants of the Ca^{2+} dyes, and the dissociation ($k_{off\text{-}DM}$) and association ($k_{on\text{-}DM}$) rate constants of DM-n.

Although our experiments were not specifically designed to test the photolysis rate by which a brief (≈50 ns) flash induces a change in affinity of DM-n, the experimental results suggest that this change occurs in less than 30 μs, in agreement with previous reports [9, 29]. There is, however, disagreement concerning the duration of the fast Ca^{2+} spike that results from the photolysis reaction. It was suggested [39], that the association rate of Ca^{2+} binding to DM-n ($k_{on\text{-}DM}$) is relatively slow (1.5×10^6 $M^{-1}s^{-1}$) and results in Ca^{2+} spikes that may last for several milliseconds. In contrast, results from our laboratory ([11, 12], this paper) and from Ellis-Davies et al. [9] suggest that $k_{on\text{-}DM}$, and consequently the Ca^{2+} spike, are at least an order of magnitude faster. In this paper we estimate that the $k_{on\text{-}DM}$ is about 0.03 μM^{-1} ms^{-1} (3×10^7 $M^{-1}s^{-1}$). The impact of this parameter on model predictions and on the interpretation of experimental data is non-trivial. It means, for example, that a Ca^{2+} spike estimated with the slower $k_{on\text{-}DM}$ to last for ≈2 ms is in reality a brief spike lasting for only ≈100 μs. The relevance of these implications motivated us to design a specific experiment (Figs. 11 and 12) to test this parameter. We found that normalized transients obtained at two, tenfold-different Fluo-3 concentrations (Fig. 12) are kinetically very similar, a result virtually impossible to predict using low values of $k_{on\text{-}DM}$.

Photolysis of DM-n generates a fast free [Ca^{2+}] transient

The free [Ca^{2+}] transients predicted by the model at pCa values greater than 9 have more similarities with a spike than a step, rising and decaying with kinetics that are considerably faster than those of the corresponding fluorescence records. According to the model, these free [Ca^{2+}] transients occur because the photolysis reaction

releases Ca^{2+} faster than the high-affinity form of DM-n rebinds it. At very low resting [Ca^{2+}] values (e.g., pCa 9), when a large fraction of DM-n is free, photolysis generates a relatively small, fast decaying free [Ca^{2+}] transient, without a significant step. This is illustrated in the inset of Fig. 8. At higher resting [Ca^{2+}] values (e.g., pCa 7; inset Fig. 14), there is less free DM-n and thus photolysis generates a larger and slower free [Ca^{2+}] transient followed by a significant step. At very high resting [Ca^{2+}] values (e.g., pCa 6, not shown), when there is essentially no free DM-n, photolysis produces a transient close to a step change in [Ca^{2+}].

Physiological implications

Data from a great number of studies involving DM-n and/or fluorescent Ca^{2+}-sensitive dyes may deserve reevaluation in light of the properties of these compounds determined in this study. We have elected to discuss below just a few examples which illustrate the broad implications that our results may import.

The limited information available concerning the time course of the fast Ca^{2+} spike generated by photolysis of DM-n was the basis of a recent disagreement concerning the regulation of single ryanodine receptor (RyR) channels. The RyR channel is a Ca^{2+}-activated intracellular Ca^{2+} release channel whose open probability peaks and then slowly decays (τ = 1.3 s) in response to flash photolysis of DM-n [15]. Other authors [21] argued that the slow decay in channel activity may simply reflect slow deactivation of the channel as the [Ca^{2+}] falls off following the fast Ca^{2+} spike. Their theoretical argument was in part based on the assumption that the Ca^{2+} spike was relatively slow [39]. Our demonstration that the Ca^{2+} spike may be more than 20 times faster than previously reported makes the Lamb and Stephenson interpretation of the data less likely. Recently, several groups have reported data showing that RyR Ca^{2+} deactivation occurs in milliseconds and therefore cannot be the mechanism responsible for the slow decay [26, 33, 34].

Local intracellular Ca^{2+} release events, called Ca^{2+} sparks, have been measured in cardiac myocytes loaded with Fluo-3. The Ca^{2+} spark is observed as a fast localized fluorescence transient which peaks in 1–2 ms and then decays with a time constant of ≈10 ms. It has been suggested [4] that the Ca^{2+} spark reflects the opening of a single RyR channel while others [27] suggest that several RyR must open in concert to generate the Ca^{2+} spark. Our data further complicate the picture, since they demonstrate that the time course of the Ca^{2+} spark may be significantly governed by the slow kinetic properties of Fluo-3. In our view, it will be important to revisit the interpretation of Ca^{2+} sparks once a proper deconvolution of the fluorescence data is performed with kinetic parameters obtained in vivo. The methodology utilized in this work is simple and well suited to measure these parameters accurately both in vivo and in vitro.

Finally, it should be mentioned that the presence of Mg^{2+} in intact cells, under physiological conditions, may significantly alter the kinetic rate constants of DM-n as determined in this paper. Consequently, careful determination of these rate constants in vivo will be necessary to evaluate the physiological effects of flash photolysis of DM-n.

Acknowledgements We thank Drs. J. Monck (UCLA) and J. Sutko (University of Nevada) for helpful comments on the manuscript. This work was supported by National Institutes of Health grant AR25201 to J.V. P.V. was supported by a Falk Cardiovascular Training Fellowship. The Vergara laboratory is part of the Cell Physiology Imaging Group, Ahmanson Laboratory of Neurobiology, Brain Research Institute, UCLA.

Appendix A

Kinetic response of a Ca^{2+}-sensitive dye to a single exponential decaying "spike"

The binding of Ca^{2+} with a dye is a simple bimolecular reaction described by the following equation:

$$[\mathrm{Ca}(t)] + [D(t)] \underset{k_{\mathrm{off}}}{\overset{k_{\mathrm{on}}}{\rightleftarrows}} [\mathrm{CaD}(t)] \tag{A1}$$

where k_{on} and k_{off} are the association and dissociation rate constants, respectively. [CaD(t)] is the concentration of Ca^{2+}–dye complex and [D(t)] is the free dye concentration, both time-dependent functions. The differential equation that describes this reaction scheme is:

$$\frac{\mathrm{d}[\mathrm{CaD}(t)]}{\mathrm{d}t} = k_{\mathrm{on}} \cdot [\mathrm{Ca}(t)] \cdot [D(t)] - k_{\mathrm{off}} \cdot [\mathrm{CaD}(t)] \tag{A2}$$

Assuming that [Ca(t)] has the form of a single exponential "spike" of amplitude $[Ca^{2+}]_{peak}$ and decay time constant τ

$$[\mathrm{Ca}(t)] = [\mathrm{Ca}^{2+}]_{\mathrm{peak}} \cdot \exp\left(\frac{-t}{\tau}\right) \tag{A3}$$

and defining $[D]_T$ as the total dye concentration and using the conservation equation $[D]_T$ = [D(t)] + [CaD(t)], the differential equation becomes:

$$\frac{\mathrm{d}[\mathrm{CaD}(t)]}{\mathrm{d}t} = k_{\mathrm{on}} \cdot [\mathrm{Ca}^{2+}]_{\mathrm{peak}} \cdot \exp\left(\frac{-t}{\tau}\right) \cdot ([D]_{\mathrm{T}} - [\mathrm{CaD}]) - k_{\mathrm{off}} [\mathrm{CaD}] \tag{A4}$$

This equation can be integrated analytically with the approximation $[D]_T$>>[CaD(t)], yielding:

$$[\mathrm{CaD}(t)] = [D]_{\mathrm{T}} \cdot k_{\mathrm{on}} \cdot [\mathrm{Ca}^{2+}]_{\mathrm{peak}} \cdot \left[\exp\left(\frac{-t}{\tau}\right) - \exp(-t \cdot k_{\mathrm{off}})\right] \cdot \left(\frac{1}{k_{\mathrm{off}} - \frac{1}{\tau}}\right) \tag{A5}$$

Quasi-delta function approximation:

If it is further assumed that $\tau << 1/k_{off}$, then:

$$[\mathrm{CaD}(t)] \approx [D]_T \cdot k_{on} \cdot [\mathrm{Ca}^{2+}]_{peak} \cdot \tau \cdot \exp(-t \cdot k_{off}) \quad \text{(A6)}$$

Finally,

$$\Delta\overline{F} = \frac{[\mathrm{CaD}(t)]}{[D]_T} \approx k_{on} \cdot [\mathrm{Ca}^{2+}]_{peak} \cdot \tau \cdot \exp(-t \cdot k_{off}) \quad \text{(A7)}$$

Appendix B

Kinetic model for flash photolysis of DM-n and detection by Ca^{2+} indicators

Definition of terms

Note that free component concentrations are functions of time (e.g. $[Ca^{2+}]=[Ca^{2+}(t)]$). The time notation has been omitted for readability.

$[Ca^{2+}]$: free calcium concentration

$[Ca^{2+}]_{t=0}$: resting (initial) free calcium concentration

$[Ca^{2+}]_T$: total calcium concentration

$[DM]_T$: total concentration of DM-n

[DM]: concentration of free DM-n

α: fraction of DM-n photolysed by a flash

[DM1]: concentration of free DM-n complex to be photolysed

[DM2]: concentration of free DM-n complex *not* photolysed

[CaDM1]: concentration of Ca^{2+}–DM-n complex to be photolysed

[CaDM2]: concentration of Ca^{2+}–DM-n complex *not* photolysed

$k_{on\text{-}DM}$: binding rate constant (on) of DM-n ($\mu M^{-1}ms^{-1}$)

$k_{off\text{-}DM}$: dissociation rate constant (off) of DM-n (ms^{-1})

K_{DM}: equilibrium dissociation constant of DM-n = $k_{off\text{-}DM}/k_{on\text{-}DM}$

$k^*_{off\text{-}DM}$: dissociation rate constant of DM-n after photolysis (ms^{-1})

$\tau_{photolysis}$: time constant of photolysis reaction

$[D]_T$: total Ca^{2+} indicator dye concentration

[D]: concentration of free Ca^{2+} indicator dye

[CaD]: concentration of Ca^{2+}–dye complex

$k_{on\text{-}D}$: binding rate constant (on) of Ca^{2+}indicator ($\mu M^{-1}ms^{-1}$)

$k_{off\text{-}D}$: dissociation rate constant (off) of Ca^{2+}indicator (ms^{-1})

t_{pulse}: point (in time) of flash pulse delivery

The model

Both DM-n and the Ca^{2+} indicator dye obey simple bimolecular binding kinetic reaction schemes.

Flash photolysis assumptions

1. The total DM-n concentration, $[DM]_T$, is arbitrarily divided into a photolyzable fraction, $[DM1]_T$, and a non-photolyzable fraction, $[DM2]_T$
2. The flash energy (α) determines the proportion of the photolyzable fraction,

$$[DM1]_T = \alpha\,[DM]_T \quad \text{(B1)}$$

3. The kinetic reaction scheme for fraction 1 *before* the flash is:

$$[\mathrm{Ca}^{2+}] + [\mathrm{DM1}] \underset{k_{off-DM}}{\overset{k_{on-DM}}{\rightleftharpoons}} [\mathrm{CaDM1}] \quad \text{(B2)}$$

4. The kinetic reaction scheme for fraction 1 *after* the flash is:

$$[\mathrm{Ca}^{2+}] + [\mathrm{DM1}] \underset{k^*_{off-DM}}{\overset{k_{on-DM}}{\rightleftharpoons}} [\mathrm{CaDM1}] \quad \text{(B2')}$$

5. The kinetic reaction scheme for fraction 2 is:

$$[\mathrm{Ca}^{2+}] + [\mathrm{DM2}] \underset{k_{off-DM}}{\overset{k_{on-DM}}{\rightleftharpoons}} [\mathrm{CaDM2}] \quad \text{(B3)}$$

6. After t_{pulse}, the photolysis reaction proceeds with a transitional dissociation rate constant, k_{trans}, given by:

$$k_{trans} = k_{off-DM} + (k^*_{off-DM} - k_{off-DM}) \cdot \left\{1 - \exp - \left[\frac{(t - t_{pulse}}{\tau_{photolysis}}\right]\right\} \quad \text{(B4)}$$

The values of $k^*_{off\text{-}DM}$ and $\tau_{photolysis}$ were set to 75 ms^{-1} and 20 μs, respectively [9, 20]

Ca^{2+} indicator kinetic scheme

$$[\mathrm{Ca}^{2+}] + [\mathrm{D}] \underset{k_{off-D}}{\overset{k_{on-D}}{\rightleftharpoons}} [\mathrm{CaD}] \quad \text{(B5)}$$

Differential equations

DM-n before the flash

$$\frac{d[\mathrm{CaDM1}]}{dt} = k_{on-DM} \cdot [\mathrm{Ca}^{2+}] \cdot [\mathrm{DM1}] - k_{off-DM} \cdot [\mathrm{CaDM1}] \quad \text{(B6)}$$

$$\frac{d[\mathrm{CaDM2}]}{dt} = k_{on-DM} \cdot [\mathrm{Ca}^{2+}] \cdot [\mathrm{DM2}] - k_{off-DM} \cdot [\mathrm{CaDM2}] \quad \text{(B7)}$$

DM-n after the flash

$$\frac{d[\mathrm{CaDM1}]}{dt} = k_{on-DM} \cdot [\mathrm{Ca}^{2+}] \cdot [\mathrm{DM1}] - k^*_{off-DM} \cdot [\mathrm{CaDM1}] \quad \text{(B8)}$$

Ca^{2+} indicator

$$\frac{d[CaD]}{dt} = k_{on-D} \cdot [Ca^{2+}] - k_{off-D} \cdot [CaD] \quad \text{(B9)}$$

Conservation equations

DM-n

$$[DM]_T = [DM1]_T + [DM2]_T \quad \text{(B10)}$$

$$[DM1]_T = [DM1] + [CaDM1] \quad \text{(B11)}$$

$$[DM2]_T = [DM2] + [CaDM2] \quad \text{(B12)}$$

Ca^{2+}-sensitive dyes and Ca^{2+}

$$[D]_T = [D] + [CaD] \quad \text{(B13)}$$

$$[Ca^{2+}]_T = [CaD] + [CaDM1] + [CaDM2] + [Ca^{2+}] \quad \text{(B14)}$$

Initial conditions

$$[Ca^{2+}] = [Ca^{2+}]_{t=0} \quad \text{(B15)}$$

$$[CaD] = \frac{[Ca]_{t=0} \cdot [D]_T}{\frac{k_{off-D}}{k_{on-D}} + [Ca]_{t=0}} \quad \text{(B16)}$$

$$[DM2] = [DM]_T \cdot (1 - \alpha) - [CaDM2] \quad \text{(B17)}$$

$$[CaDM2] = \frac{[Ca^{2+}]_{t=0} \cdot [DM]_T \cdot (1-\alpha)}{\left(\frac{k_{off-DM}}{k_{on-DM}} + [Ca^{2+}]_{t=0}\right)} \quad \text{(B18)}$$

Numerical integration method: Fourth-order Runge-Kutta

References

1. Adams SR, Kao JPY, Grynkiewicz G, Minta A, Tsien RY (1988) Biologically useful chelators that release Ca^{2+} upon illumination. J Am Chem Soc 110:3212–3220
2. Alvarez-Leefmans FJ, Rink TJ, Tsien RY (1981) Free calcium ions in neurones of *Helix aspersa* measured with ion-selective micro-electrodes. J Physiol (Lond) 315:531–548
3. Bers DM (1982) A simple method for the accurate determination of free $[Ca^{2+}]$ in Ca-EGTA solutions. Am J Physiol 242:404–408
4. Cannell MB, Cheng HP, Lederer WJ (1994) Spatial non-uniformities in $[Ca^{2+}]_i$ during excitation-contraction coupling in cardiac myocytes. Biophys J 67:1942–1956
5. Cifuentes F, Escobar AL, Vergara JL (1995) Calcium Orange-5N: a low affinity indicator able to track the fast release of calcium in skeletal muscle fibers. Biophys J 68:419a
6. DiPolo R, Rojas H, Vergara J, Lopez R, Caputo C (1983) Measurements of intracellular ionized Ca^{2+} in squid giant axons using Ca-selective electrodes. Biochim Biophys Acta 728:311–318
7. Delaney KR, Zucker RS (1990) Calcium released by photolysis of DM-nitrophen stimulates transmitter release at squid giant synapse. J Physiol (Lond) 426:473–498
8. Eberhard M, Erne P (1989) Kinetics of calcium binding to fluo-3 determined by stopped-flow fluorescence. Biochem Biophys Res Commun 123:309–314
9. Ellis-Davies GCR, Kaplan JH, Barsotti RJ (1996) Laser photolysis of caged calcium: rates of calcium release by Nitrophenyl-EGTA and DM-Nitrophen. Biophys J 70:1006–1016
10. Escobar AL, Monck J, Fernandez JM, Vergara JL (1994) Localization of the site of Ca^{2+} release at the level of a single sarcomere in skeletal muscle fibers. Nature 367:739–741
11. Escobar AL, Cifuentes F, Vergara JL (1995) Detection of Ca^{2+} transients elicited by flash photolysis of DM-Nitrophen with a fast indicator. FEBS Lett 364:335–338
12. Escobar AL, Velez P, Cifuentes F, Fill M, Vergara JL (1995) Kinetic properties of calcium indicators in response to calcium spikes. Biophys J 68:418a
13. Fryer MW, Zucker RS (1993) Ca^{2+} dependent inactivation of Ca^{2+} current in *Aplysia* neurons: kinetic studies using photolabile Ca^{2+} chelators. J Physiol (Lond) 464:501–528
14. Grynkiewicz G, Poenie M, Tsien RY (1985) A new generation of Ca^{2+} indicators with greatly improved fluorescence properties. J Biol Chem 260:3440–3450
15. Gyorke S, Fill M (1993) Ryanodine receptor adaptation-control mechanism of Ca^{2+}-induced Ca^{2+} release in heart. Science 260:807–809
16. Gyorke S, Fill M (1994) Ca^{2+}-induced Ca^{2+}-release in response to a flash photolysis. Science 263:987–988
17. Gyorke S, Velez P, Suarez-Isla B, Fill M (1994) Activation of single cardiac and skeletal ryanodine receptor channels by flash photolysis of caged Ca^{2+}. Biophys J 66:1879–1886
18. Kaplan JH (1990) Special topic – caged compounds in cellular physiology – introduction. Annu Rev Physiol 52:853–855
19. Kaplan JH (1990) Photochemical manipulation of divalent cation levels. Annu Rev Physiol 52:897–914
20. Kaplan JH, Ellis-Davies GC (1988) Photolabile chelators for the rapid photorelease of divalent cations. Proc Natl Acad Sci 85:6571–6575
21. Lamb GD, Stephenson DG (1995) Activation of ryanodine receptors by flash photolysis of caged Ca^{2+} Biophys J 68: 946–948
22. Lamb GD, Fryer MW, Stephenson DG (1994) Ca^{2+}-induced-Ca^{2+} release in response to flash photolysis. Science 263:986–987
23. Lando L, Zucker RS (1989) Caged calcium in *Aplysia* pacemaker neurons. Charaterization of the calcium activated potassium and nonspecific cation currents. J Gen Physiol 93:1017–1060
24. Lando L, Zucker RS (1994) Ca^{2+} cooperativity in neurosecretion measured using photolabile Ca^{2+} chelators. J Neurophysiol 72:825–830
25. Lattanzio FA, Bartschat DK (1991) The effect of pH on rate constants, ion selectivity and thermodynamic properties of fluorescent calcium and magnesium indicators. Biochem Biophys Res Commun 177:184–191
26. Laver D, Curtis B (1996) Rapid solution change activates ryanodine receptors within 30 ms. Biophys J 70:387a
27. Lipp P, Niggli E (1996) Submicroscopic calcium signals as fundamental events of excitation-contraction coupling in guinea-pig cardiac myocytes. J Physiol (Lond) 492:31–38
28. Lopez JR, Alamo L, Caputo C, Dipolo R, Vergara J (1983) Determination of ionic calcium in frog skeletal muscle fibers. Biophys J 43:1–4
29. McCray JA, Fidler-Lim N, Ellis-Davies GC, Kaplan JH (1992) Rate of release of Ca^{2+} following laser photolysis of the DM-nitrophen-Ca^{2+} complex. Biochemistry 31:8856–8861
30. Minta A, Kao JPY, Tsien RY (1989) Fluorescence indicators for cytosolic calcium based on rhodamine and fluorescein chromophores. J Biol Chem 264:8171–8178
31. Morad M, Davies NW, Kaplan JH, Lux HD (1988) Inactivation and block of calcium channels by photo-released Ca^{2+} in dorsal root ganglion neurons. Science 241:842–844

32. Riecke F, Schwartz EA (1996) Asynchronous transmitter release: control of exocytosis and endocytosis at the salamander rod synapse. J Physiol (Lond) 493:1–8
33. Sitsapesan R, Montgomery RA, Williams AJ (1995) New insights into the gating mechanisms of cardiac ryanodine receptors revealed by rapid changes in ligand concentration. Circ Res 77:765–772
34. Velez P, Lokuta AJ, Valdivia HH, Gyorke S, Fill M (1996) Adaptation of cardiac ryanodine receptor channels. Biophys J 70:165a
35. Vergara LJ, Escobar AL (1993) Detection of calcium transients in skeletal muscle fibers using the low affinity dye Calcium-Green-5N. Biophys J 65:37a
36. Vergara J, Di Franco M, Compagnon D, Suarez-Isla B (1991) Imaging of calcium transients in skeletal muscle fibers. Biophys J 59:12–24
37. Wilson T (1990) In: Wilson T (ed) Confocal microscopy. Academic, New York
38. Zucker RS (1992) Effects of photolabile calcium chelators on fluorescent calcium indicators. Cell Calcium 13:29–40
39. Zucker RS (1993) The calcium concentration clamp: spikes and reversible pulses using the photolabile chelator DM-nitrophen. Cell Calcium 14:87–100
40. Zucker RS (1994) Photorelease techniques for raising or lowering intracellular Ca^{2+}. Methods Cell Biol 40:31–63